Polyelectrolyte Multilayers of Diblock Copolymer Micelles with Temperature-Responsive Cores

ARTICLE *in* LANGMUIR · JANUARY 2011

Impact Factor: 4.46 · DOI: 10.1021/la1038014 · Source: PubMed

3 AUTHORS, INCLUDING:

Zhichen Zhu
Stevens Institute of Technology
10 PUBLICATIONS **269** CITATIONS
SEE PROFILE

Svetlana Sukhishvili
Stevens Institute of Technology
134 PUBLICATIONS **4,810** CITATIONS
SEE PROFILE

Langmuir
Article
pubs.acs.org/Langmuir

Polyelectrolyte Multilayers of Diblock Copolymer Micelles with Temperature-Responsive Cores

Li Xu, Zhichen Zhu, and Svetlana A. Sukhishvili*

Department of Chemistry, Chemical Biology and Biomedical Engineering, Stevens Institute of Technology, Hoboken, New Jersey 07030, United States

Received September 22, 2010. Revised Manuscript Received November 22, 2010

We report on assembly and stimuli-response behavior of layer-by-layer (LbL) films of pH- and temperature-responsive cationic diblock copolymer micelles (BCMs) of poly(2-(dimethylamino)ethyl methacrylate)-*block*-poly(*N*-isopropylacrylamide) (PDMA-*b*-PNIPAM) and a linear polyanion polystyrene sulfonate (PSS). As a function of solution pH at temperatures above lower critical solution temperature (LCST) of PNIPAM, PDMA-*b*-PNIPAM micelles have been demonstrated earlier to exhibit an abrupt change in micellar aggregation number and hydrodynamic size between larger and smaller BCMs (LBCMs and SBCMs, respectively). Here, LBCMs or SBCMs were included within LbL films through self-assembly with a polyanion, and film pH and temperature responses were studied using ellipsometry and atomic force microscopy (AFM). Both types of micelle preserved their micellar morphology when adsorbed at the surface of oxidized silicon wafers coated with PSS-terminated precursor layer at a constant pH. Response of adsorbed BCMs to temperature and pH variations was strongly dependent on whether or not BCMs were coated with the PSS layer. While monolayers of LBCMs lost their original dry morphology in response to pH or temperature variations, depositing a PSS layer atop LBCMs inhibited such irreversible restructuring. As a result of wrapping around and strong binding of PSS chains with LBCM micelles, BCM/PSS assemblies preserved their original dry state morphology despite the application of pH and temperature triggers. However, the wet-state film response to pH and temperature stimuli was drastically different. Swelling of BCM/PSS multilayers was strongly affected by temperature but was almost independent of pH due to neutralization of BCM PDMA's coronal charge with PSS. Cycling the temperature below and above PNIPAM's LCST caused PNIPAM chains within BCM cores to swell or collapse, resulting in reversible swelling transitions in the entire BCM/PSS assemblies. Temperature-controlled switching between the hydrophobic and hydrophilic state of assembled micellar cores was also used to regulate the release of a micelle-loaded hydrophobic pyrene dye, whose release rate increased at temperatures below PNIPAM's LCST.

Introduction

Stimuli-responsive films that control adhesion, wetting, and binding or release of functional molecules at surfaces are promising candidates for applications in separation, sensing, and biomedicine. A powerful yet simple technique to fabricate stimuli-responsive thin films is the layer-by-layer (LbL) sequential adsorption technique.[1−7] The technique enables construction of polymer films with nanoscopically controlled thickness, diverse chemical composition, and capacity to adhere to a wide range of surfaces of arbitrary shape. One important stimulus most often explored with LbL polyelectrolyte multilayer films (PEMs) is the solution pH that can affect film swelling,[8] composition,[9] and the capacity to retain and release functional guest molecules.[10] Other important relevant stimuli include temperature and/or light. Temperature-responsive LbL films have been constructed earlier by assembly of temperature-responsive random copolymers,[11,12] while light responsiveness has been imparted to PEMs through the use of polymers containing photochromic azobenzene moieties[13] or gold nanoparticles[14] as LbL building blocks.

Recent years have seen increased interest in endowing PEMs with enhanced functionality through the use of block copolymers as film constituents. This development was largely enabled by recent advances in polymer synthesis, in particular by progress in controlled radical polymerization techniques affording a wide range of amphiphilic diblock copolymers.[15,16] In aqueous solution, such diblock copolymers self-assemble into diblock copolymer micelles (BCMs) composed of water-soluble hydrophilic coronae and hydrophobic cores, which are known to incorporate hydrophobic materials such as dyes[17] or inorganic particles.[18] The high loading capacity of BCM hydrophobic cores for guest molecules is specifically attractive in using BCMs as building blocks for constructing LbL films.

Multilayers of BCMs with permanently hydrophobic cores have been reported by several groups. Using two types of polyelectrolyte

*Corresponding author. E-mail: ssukhish@stevens.edu.

(1) Decher, G. *Science* **1997**, *277*, 1232.
(2) Hammond, P. T. *Adv. Mater.* **2004**, *16*, 1271.
(3) Ramey, M. B.; Hiller, J.; Rubner, M. F.; Tan, C. Y.; Schanze, K. S.; Reynolds, J. R. *Macromolecules* **2005**, *38*, 234.
(4) Markarian, M. Z.; Mousallem, M. D.; Jomaa, H. W.; Schlenoff, J. B. *Biomacromolecules* **2007**, *8*, 59.
(5) Stockton, W. B.; Rubner, M. F. *Macromolecules* **1997**, *30*, 2717.
(6) Sukhishvili, S. A.; Granick, S. *J. Am. Chem. Soc.* **2000**, *122*, 9550.
(7) Yang, S. G.; Zhang, Y. J.; Wang, L.; Hong, S.; Xu, J.; Chen, Y. M.; Li, C. M. *Langmuir* **2006**, *22*, 338.
(8) Chung, A. J.; Rubner, M. F. *Langmuir* **2002**, *18*, 1176.
(9) Izumrudov, V A.; Kharlampieva, E.; Sukhishvili, S. A. *Biomacromolecules* **2005**, *6*, 1782.
(10) Lee, D.; Nolte, A. J.; Kunz, A. L.; Rubner, M. F.; Cohen, R. E. *J. Am. Chem. Soc.* **2006**, *128*, 8521.
(11) Jaber, J. A.; Schlenoff, J. B. *Macromolecules* **2005**, *38*, 1300.
(12) Serpe, M. J.; Yarmey, K. A.; Nolan, C. M.; Lyon, L. A. *Biomacromolecules* **2005**, *6*, 408.
(13) Kumar, S. K.; Hong, J.-D. *Langmuir* **2008**, *24*, 4190.
(14) Wang, S. B.; Li, C.; Chen, F. E.; Shi, G. Q. *Nanotechnology* **2008**, *18*, 185707.
(15) Chen, G.; Hoffman, A. S. *Nature* **1995**, *373*, 49.
(16) Matyjaszewski, K.; Xia, J. *Chem. Rev.* **2001**, *101*, 2921.
(17) Ma, N.; Zhang, H. Y.; Song, B.; Wang, Z. Q.; Zhang, X. *Chem. Mater.* **2005**, *17*, 5065.
(18) Kim, B.-S.; Qiu, J. M.; Wang, J. P.; Taton, T. A. *Nano Lett.* **2005**, *5*, 1987.

micelles with glassy polystyrene cores and anionic and cationic coronae, Cho et al. demonstrated self-assembly of all-micelle multilayer films whose porosity could be controlled by ionization of coronal weak polyelectrolyte chains.[19] Qi et al. also reported all-BCM LbL films built from cationic and anionic micelles with glassy cores and used them for embedding two different types of hydrophobic dyes.[20] Hydrogen-bonded multilayers were also constructed using BCMs with permanently hydrophobic cores, and pH-induced disintegration of the LbL film was used to deliver micelle-loaded therapeutic molecules from surfaces.[21] Self-assembly of BCMs with biodegradable linear polyelectrolytes has also been demonstrated to achieve controlled delivery of BCM-embedded drugs from surfaces via erosion of the PEM films.[22] A useful pH-response function can also be added to such self-assemblies by introducing a pH-sensitive hydrolyzable linkage between a drug and a micelle.[23]

In contrast to BCMs with permanently hydrophobic cores, another interesting type of BCMs includes micelles susceptible to environmental stimuli. Cores of such micelles are typically plasticized and can disintegrate or restructure in aqueous solutions in response to variations of solution pH,[24,25] temperature,[26−28] ionic strength,[29,30] or light.[31] Relatively few reports have demonstrated incorporation of responsive micelles of this type within multilayers. Biggs et al. reported that two types of BCMs with oppositely charged coronae and pH-responsive cores can be coated on the surface of silica particles, giving colloids with high loading capacities for hydrophobic dyes.[32] Nguyen et al. have also demonstrated the use of PEMs of linear−dendritic BCMs with collapsed poly(propylene oxide) (PPO) cores for extended release of antibacterial agents.[33] These studies, however, did not address environmental response of such films. In our recent work, we reported on hydrogen-bonded films of diblock copolymer micelles with poly(*N*-isopropylacrylamide) (PNIPAM) cores that exhibit lower critical solution temperature (LCST) behavior. As a result of temperature-triggered collapse and rehydration of micellar cores, the films showed pronounced, reversible temperature-triggered swelling transitions and temperature-controlled release of embedded small molecules.[34] These earlier reported hydrogen-bonded films were stable only in acidic environments, however, and disintegrated at neutral pH values.[34] Very recently, the films stable in a wide range of pH and exhibiting large-amplitude temperature-triggered swelling transitions were electrostatically assembled using poly(acrylic acid) and cationic triblock copolymer micelles with temperature-responsive PPO cores.[35] It remained unclear, however, whether temperature-responsive, pH-stable LbL assemblies can be constructed using diblock rather than triblock copolymer micelles.

Here, we present the first study of responsive properties of electrostatically assembled multilayer films containing diblock copolymer micelles with temperature-responsive cores. The solution behavior of block copolymer used in LbL assembly—poly(2-(dimethylamino)ethyl methacrylate)-*block*-poly(*N*-isopropylacrylamide) (PDMA-*b*-PNIPAM)—was studied in our earlier work.[36] At temperatures above LCST of PNIPAM blocks, the copolymer solutions demonstrate micelle-to-micelle phase transition that occurs in a narrow pH range, and micelles disintegrate to unimers at temperature below PNIPAM's LCST.[36] In this study, we were interested to extend our studies to adsorbed layers of such micelles and contrast the responsive behavior of PDMA-*b*-PNIPAM BCMs in solution and at surfaces. We showed that self-assembly of PDMA-*b*-PNIPAM micelles with polystyrene sulfonate (PSS) at surfaces inhibited pH response of assembled BCMs, while preserving micellar temperature response. Preserving micellar morphology was central to endowing reversible swelling transitions, as well as controlled drug release properties to the BCM/PSS films. As a result of temperature-triggered changes in the uptake of water within micellar cores, BCM/PSS films exhibited temperature-induced, largely reversible, swelling transitions, indicating kinetic freezing of PDMA/PSS ionic pairing and intertwining of PSS chains and BCMs within layered polymer constructs. We also show the ability of BCM/PSS films to control the retention and release of hydrophobic molecules within/from the core of assembled BCMs in response to temperature variations.

Experimental Section

Materials. The PDMA-*b*-PNIPAM block copolymer was synthesized by atom transfer radical polymerization which was described elsewhere.[36] The weight-average molecular weights of PDMA and PNIPAM blocks were 15 and 24 kDa, respectively, as determined by a combination of gel permeation chromatography (GPC) and ^{1}H NMR. The GPC studies of single PDMA block and block copolymer performed in tetrahydrofuran have also revealed polydispersity indices of 1.10 and 1.25 for the PDMA block and the PDMA-*b*-PNIPAM copolymer, respectively. The block copolymer is abbreviated as $PDMA_{57}$-*b*-$PNIPAM_{97}$, where the subscript denotes the average number of monomer units in each copolymer block.

Ultrapure Milli-Q water (Millipore) with a resistivity higher than 18 MΩ/cm was used in all experiments. Sodium salt of PSS with M_w = 500 000 g mol^{-1} was purchased from Scientific Polymer Products, Inc. Branched polyethylenimine (BPEI) with M_w = 25 000 g mol^{-1} was purchased from Aldrich. All other chemicals were purchased from Aldrich and used without further purification. Silicon wafers with ⟨100⟩ orientation were purchased from Cemat Silicon S.A., Poland.

Preparation of PDMA-*b*-PNIPAM Micelles. At temperatures higher than LCST of PNIPAM, PDMA-*b*-PNIPAM copolymer forms spherical micelles of two distinct aggregation numbers and sizes, i.e., larger BCMs (LBCMs) and smaller BCMs (SBCMs) depending on the value of solution pH.[36] Here, pH 6 and pH 4 were chosen for deposition of LBCMs and SBCMs, respectively. To prepare LBCMs and SBCMs, diblock copolymer was first dissolved in 0.01 M phosphate buffer solution at a concentration of 0.2 mg/mL at pH 4 for 12 h at 25 °C, where the copolymer was molecularly dissolved. While phosphate ions can decrease the LCST of PNIPAM and PDMA as a result of binding

(19) Cho, J.; Hong, J.; Char, K.; Caruso, F. *J. Am. Chem. Soc.* **2006**, *128*, 9935.
(20) Qi, B.; Tong, X.; Zhao, Y. *Macromolecules* **2006**, *39*, 5714.
(21) Kim, B.-S.; Park, S. W.; Hammond, P. T. *ACS Nano* **2008**, *2*(2), 386.
(22) Kim, B.-S.; Smith, R. C.; Poon, Zh.; Hammond, P. T. *Langmuir* **2009**, *25*, 14086.
(23) Kim, B.; Lee, H.; Min, Y. H.; Poon, Z. Y.; Hammond, P. T. *Chem. Commun.* **2009**, *28*, 4194.
(24) Gillies, E. R.; Fréchet, J. M. J. *Bioconjugate Chem.* **2005**, *16*(2), 361.
(25) Schilli, C. M.; Zhang, M. F.; Rizzardo, E.; Thang, S. H.; Chong, Y. K.; Edwards, K.; Karlsson, G.; Müller, A. H. *Macromolecules* **2004**, *37*, 7861.
(26) André, X.; Zhang, M. F.; Müller, A. H. *Macromol. Rapid Commun.* **2005**, *26*, 558.
(27) Lee, H.-I.; Lee, J. A.; Poon, Z. Y.; Hammond, P. T. *Chem. Commun.* **2008**, 3726.
(28) De, P.; Gondi, S. R.; Sumerlin, B. S. *Biomacromolecules* **2008**, *9*, 1064.
(29) Bütün, V.; Armes, S. P.; Billingham, N. C.; Tuzar, Z.; Rankin, A.; Eastoe, J.; Heenan, R. K. *Macromolecules* **2001**, *34*, 1503.
(30) Rodríguez-Hernández, J.; Lecommandoux, S. *J. Am. Chem. Soc.* **2005**, *127*, 2026.
(31) Lee, H.-I.; Wu, W.; Oh, J. K.; Mueller, L.; Sherwood, G.; Peteanu, L.; Kowalewski, T.; Matyjaszewski, K. *Angew. Chem., Int. Ed.* **2007**, *46*(14), 2453.
(32) Biggs, S.; Sakai, K.; Addison, T.; Schmid, A.; Armes, S. P.; Vamvakaki, M.; Bütün, V.; Webber, G. *Adv. Mater.* **2007**, *19*, 247.
(33) Nguyen, P. M.; Zacharia, N. S.; Verploegen, E.; Hammond, P. T. *Chem. Mater.* **2007**, *19*, 5524.
(34) Zhu, Z. C.; Sukhishvili, S. A. *ACS Nano* **2009**, *3*, 3595.
(35) Tan, W. S.; Cohen, R. E.; Rubner, M. F.; Sukhishvili, S. A. *Macromolecules* **2010**, *43*, 1950.
(36) Xu, L.; Zhu, Z. C.; Borisov, O. V.; Zhulina, E. B.; Sukhishvili, S. A. *Phys. Rev. Lett.* **2009**, *103*(11), 118301.

with amine groups, the literature data[37,38] and our control experiments showed that this effect is pronounced only at large concentrations (0.1−1 M) of phosphate salts, and the solution behavior of PDMA-*b*-PNIPAM micelles was not affected by the low concentration (0.01 M) of phosphate buffer used in our work. The solution was then filtered using a syringe filter with a 0.45 μm pore size (nylon, sterile, purchased from Fisher Scientific) to remove dust and/or impurities. When needed, the solution pH was adjusted to 6 or 4 using 0.1 M aqueous NaOH. The formation of copolymer micelles was accomplished by heating the solution to 45 °C for 2 h.

Deposition of BCM/PSS Films. Silicon wafers were precleaned by exposure to UV radiation for 2 h, immersed in concentrated H_2SO_4 for 15 min, rinsed with Milli-Q water, immersed in 0.1 M NaOH solution for 5 min, and finally thoroughly rinsed with Milli-Q water prior to film deposition. Silicon wafers were primed with BPEI/PSS precursor layers deposited by immersing the precleaned silicon substrates in a 0.2 mg/mL BPEI aqueous solution adjusted to pH 9 and 25 °C for 12 h, followed by rinsing with Milli-Q water and dipping into 0.2 mg/mL PSS solution in pH 6 0.01 M phosphate buffer at 45 °C for 15 min and rinsing. The dry ellipsometric thickness of the BPEI/PSS film was 3.0 ± 0.1 nm. Multilayer films were then constructed by sequential deposition of PDMA-*b*-PNIPAM micelles and PSS. For LBCM/PSS and SBCM/PSS multilayer films, pH of all solutions was controlled at 6 and 4, respectively. Multilayer films were deposited from 0.2 mg/mL polymer solutions at 45 °C, allowing 15 min for polymer adsorption and applying two washing cycles with 0.01 M phosphate buffer, followed by drying with a nitrogen stream after each deposition step. Multilayer names are abbreviated as $(BCM/PSS)_n$, where the subscript n represents the number of deposition cycles.

Application of pH and Temperature Stimuli. The pH response of LBCM monolayers and LBCM/PSS bilayer films deposited at pH 6 was measured by dipping films into 0.01 M phosphate buffer solution at pH 4 and 45 °C for different time intervals, followed by immersing in 0.01 M phosphate buffer solution at pH 6 at the same temperature. To probe temperature response, LBCM monolayers and LBCM/PSS films were immersed into 0.01 M phosphate buffer solution at pH 6 and 25 °C, followed by dipping in the same buffer at 45 °C. Similar procedures were used to explore the pH and temperature responses of SBCM monolayers and SBCM/PSS bilayer films, deposited at pH 4, with pH 6 dipping solution used first and pH 4 later (opposite to the dipping sequence used in LBCM film studies).

Preparation of Pyrene-Loaded LbL Films and Measurements of Pyrene Release. Pyrene was used as a hydrophobic probe to detect growth, drug-loading, and release properties of LBCM/PSS multilayer films. Pyrene solution was prepared by dissolving 0.1 g of pyrene in 2 mL of acetone and adding into 100 mL of buffered Milli-Q water. After evaporation of acetone, the solution was sonicated at 25 °C for 2 h and allowed to equilibrate overnight at room temperature. The resulting solution was filtered using a syringe filter with a 0.45 μm pore size to obtain saturated aqueous pyrene solution with a concentration of $\sim 6 \times 10^{-7}$ M.

All deposition solutions were prepared by dissolving polymers (at concentration 0.2 mg/mL) in the saturated aqueous pyrene solution. Saturated aqueous pyrene solution was also used as a rising solution. Prior to deposition, the polymer solutions were equilibrated with stirring overnight, adjusted to pH 6, and preheated in a water bath at 45 °C for 5 h. In the case of PDMA-*b*-PNIPAM solutions, this procedure enabled formation of LBCMs and inclusion of pyrene within hydrophobic micellar cores. Films were deposited on glass slides (Gold Seal Products, Inc.) cut to fit a quartz cuvette for fluorescence measurements and coated by the BPEI/PSS precursor layer using the procedure described above.

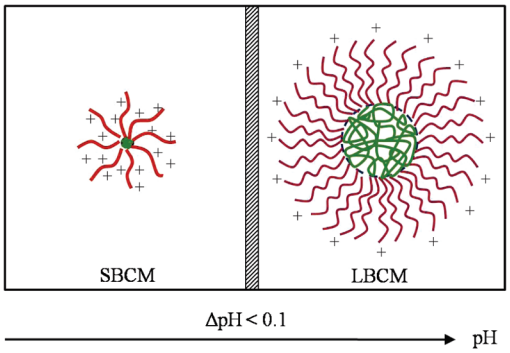

Figure 1. Schematic representation of the pH-controlled micellization of PDMA-*b*-PNIPAM in solutions at temperature higher than PNIPAM's LCST. The vertical line indicates a narrow pH region separating SBCMs and LBCMs.[36]

For fluorescence experiments with dry multilayer films, the glass slides with deposited multilayers were inserted within an empty quartz cuvette at 45° angle with the incident beam. For the dye release experiments, the glass slides with (pyrene-loaded LBCM/PSS)$_{10}$ ((LBCM^{pyr}/PSS)$_{10}$) films were immersed into a quartz cuvette containing 2 mL of 0.01 M phosphate buffer solution with desired temperature (25, 35, 40, or 45 °C) and pH (4, 6, or 7.5). After a certain immersion time, the glass substrates were withdrawn from the solutions, and fluorescence intensity of the solutions was then detected.

Ellipsometry. The thickness of dry and solution-exposed multilayers was monitored using a custom-built, single-wavelength, phase-modulated ellipsometer at 65° angle of incidence. The instrument setup and measurement procedure can be found in our earlier publication.[39] For dry films, the refractive indices for SiO_2 layer on a silicon substrate and dry polymer films were set at 1.456 and 1.500, respectively. For measurements of the degree of swelling of LbL films, a home-built fluid cell was used. During *in situ* measurements, the refractive index of 1.333 was used for water and 0.01 M phosphate buffer solutions, while the refractive index of LbL films was not set at a constant value. The dry thickness of the precursor layer was 3.0 ± 0.1 nm. This value was always subtracted from the ellipsometry measurements of dry films. Measurements of film swelling were done after incubating the films for 5 min in pH- and temperature-adjusted 0.01 M buffer solutions.

Atomic Force Microscopy (AFM). AFM was used to characterize morphology of dry and solution-immersed BCM/PSS films using an NSCRIPTOR™ dip pen nanolithography system (Nanoink). For dry films, the instrument operated in the ac (tapping) mode using P-MAN-SICC-0 AFM cantilevers (Pacific Nanotechnology, Inc.) with a nominal force constant of 40 N/m. For films in aqueous solution, the AFM instrument operated in the contact mode using P-MAN-SICT-0 AFM cantilevers (Pacific Nanotechnology, Inc.) with a nominal force constant of 0.2 N/m.

Fluorescence Spectroscopy. Fluorescence spectra were taken with a Shimadzu RF-1501 spectrofluorometer using a quartz cuvette with 10 mm path length (Fisher Scientific) at excitation wavelength $\lambda_{ex} = 333$ nm.

Results and Discussion

Self-assembly of PDMA-*b*-PNIPAM copolymers in solution has been reported in our prior publication.[36] The main finding in this prior work is schematically summarized in Figure 1. In particular, at temperatures above PNIPAM's LCST of 32−35 °C, PDMA-*b*-PNIPAM having the ratio of PDMA-to-PNIPAM lengths from 0.5 to 1 formed spherical micelles, with aggregation

(37) Zhang, Y. J.; Furyk, S.; Bergbreiter, D. E.; Cremer, P. S. *J. Am. Chem. Soc.* **2005**, *127*, 14505.
(38) Zhang, Y. J.; Premer, P. S. *Curr. Opin. Chem. Biol.* **2006**, *10*, 658.
(39) Pristinski, D.; Kozlovskaya, V.; Sukhishvili, S. A. *J. Opt. Soc. Am. A* **2006**, *23*, 2639.

number of PDMA-*b*-PNIPAM BCMs strongly dependent on solution pH. Changes in the aggregation number and the micellar size were abrupt, and micelles of two distinct sizes, i.e., SBCMs ($R_h = 10 \pm 2$ nm) and LBCMs ($R_h = 35 \pm 3$ nm), existed at lower and higher pH values, respectively, with transitions occurring in a narrow pH range, $\Delta pH < 0.1$. In a specific case of $PDMA_{57}$-*b*-$PNIPAM_{97}$ in 0.01 M phosphate buffer solutions of the BCM at 45 °C, transitions between weakly charged LBCM with aggregation number (N_{agg}) of 55 ± 3 and strongly charged SBCM with N_{agg} of 10 ± 0.5 were observed at pH ~5.2. The critical pH value for the transition is dependent on several factors, including temperature, molecular weights of copolymer blocks, and pK_a of polymer chains in the micellar corona (pK_a of PDMA is 6.8). In our prior publication, we presented a combined experimental and theoretical study of such transitions.[36] Here, we aimed to include PDMA-*b*-PNIPAM micelles within LbL films via electrostatic assembly with a linear polyanion and to examine response behavior of the constructed films. Because of the obvious advantages offered by the larger micelles for AFM imaging, morphological studies of the films are primarily demonstrated with LBCM/PSS assemblies, while ellipsometry of dry and swollen films, including the results shown in the Supporting Information, has been performed with LBCM/PSS and SBCM/PSS films.

pH and Temperature Responses of Dry $PDMA_{57}$-*b*-$PNIPAM_{97}$ BCM/PSS Assemblies: Monolayers vs Bilayers. In 0.01 M phosphate buffer solutions at pH 6 and 45 °C, LBCMs had R_h of ~35 nm and ζ-potential of ~+18 mV. The positive charge of PDMA coronal chains of LBCMs assured adsorption of micelles at the negatively charged, BPEI/PSS precursor-coated surfaces of silicon wafers and enabled binding of BCMs with PSS. Previously, morphological restructuring in monolayers of different BCMs with PDMA coronae and pH-dissolvable poly (2-diethylamino)ethyl methacrylate (PDEA) cores have been studied at surfaces of bare mica and silica, rather than at surfaces precoated with a BPEI/PSS precursor layer.[40] Images in Figures 2 and 3a show morphology of LBCM monolayers and LBCM/PSS bilayers as deposited at pH 6 and dried.

Micellar morphology was clearly retained after adsorption of LBCM micelles within a monolayer as well as after deposition of a top PSS layer. Note that the deposition pH of 6 was 0.8 pH units higher that the critical pH value of 5.2 required for micellar restructuring. Since this was obviously larger than the expected pH lowering from the bulk value near the PSS-topped precursor structure (due to the effect of local pH changes in the vicinity of charged surfaces[41]), the surface micelles remained large in size and did not restructure to smaller micelles upon adsorption. The saturated surface coverage achieved for the micellar monolayer adsorbed from 0.2 mg/mL solutions for 15 min was only ~40% of the surface area. This coverage did not increase when PDMA-*b*-PNIPAM concentration was increased from 0.2 to 1 mg/mL, nor with deposition time up to 1 h. The average intermicellar distance in the saturated layer was relatively large, i.e., 50 ± 10 nm. A similar average distance between micelles was reported by Sakai et al.[40] for the case of monolayers of responsive micelles with different pH-responsive cores but the same PDMA coronal blocks. The authors explained the large intermicellar distances by an increased micellar footprint at the surface resulting from interactions of coronal blocks with the substrate. Similarly, in our case, the average lateral radius of micelles increased from 35 ± 3 nm in bulk solution to 60 ± 15 nm after adsorption at the surface. These

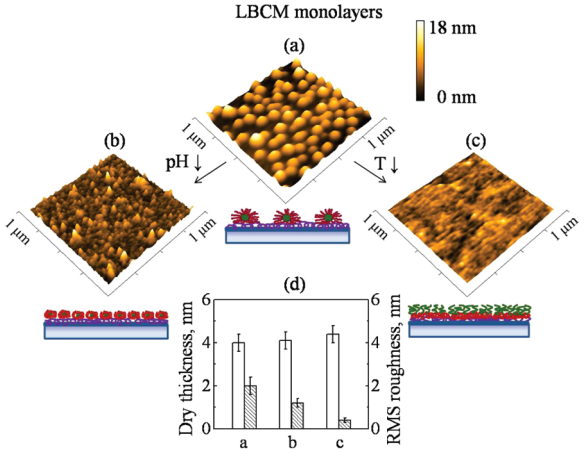

Figure 2. pH and temperature responses of LBCM monolayers with dry ellipsometric thickness of 4.0 ± 0.3 nm deposited on BPEI/PSS precursor layer measured by AFM of dry films. Films were deposited in 0.01 M phosphate buffer solution at pH 6, 45 °C (a), and then immersed in 0.01 M phosphate buffer solution at pH 4, 45 °C (b) or pH 6, 25 °C (c) for 4 h, respectively. Scale: 1 μm × 1 μm. (d) Comparison of ellipsometric thickness (blank) and rms roughness (filled) of dry LBCM monolayer films after treatments.

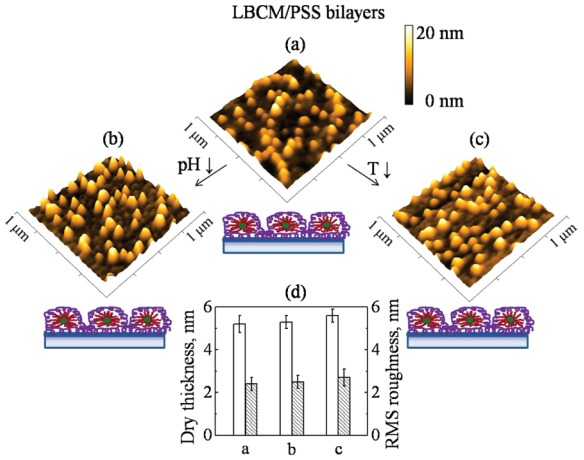

Figure 3. pH and temperature responses of dry LBCM/PSS bilayers with ellipsometric thickness of 5.2 ± 0.4 nm adsorbed at a BPEI/PSS precursor film as monitored by tapping mode AFM. Films were deposited at pH 6, 45 °C (a), followed by incubation in 0.01 M phosphate buffer solution at pH 4, 45 °C (b) or pH 6, 25 °C (c) for 4 h. Scale: 1 μm × 1 μm. (d) Comparison of ellipsometric thickness (blank) and rms roughness (filled) of dry LBCM/PSS bilayer films after treatments.

changes reflect micellar flattening caused by strong interactions of PDMA coronal chains with PSS chains in the precursor layer. The height of dry adsorbed micelles of ~10 nm also reflects such interaction-induced flattening as well as the removal of water from swollen micelles as a result of drying. Interestingly, Sakai et al.[40] showed that the micellar footprint in the adsorbed layer increased with an increase in anchoring strength between coronal blocks and the surface. Unlike silica and mica surfaces used in the above study, our surfaces were decorated with PSS—a polymer known to strongly bind with polycations. Therefore, the intermicellar distance found in this work was higher than that reported for binding of micelles with PDMA coronae onto silica surface.

Figure 2 contrasts the effects of pH and temperature on LBCM monolayer film morphology and film thickness. Application of both pH and temperature triggers dramatically changed surface

(40) Sakai, K.; Smith, E. G.; Weber, G. B.; Schatz, C.; Wanless, E. J.; Bütün, V.; Armes, S. P.; Biggs, S. *Langmuir* **2006**, *22*, 5328.
(41) Goldstein, L.; Levin, Y.; Katchalski, E. *Biochemistry* **1964**, *3*, 1913.

morphology and reduced root-mean-square (rms) roughness, but much smoother films were obtained upon lowering temperature. After deposition and after exposure to solutions of various pH and temperature, the dry BPEI/PSS precursor layer maintained an average thickness 3 ± 0.1 nm and a smoothness of 0.2 ± 0.1 nm (see Figure S1). When PDMA-*b*-PNIPAM BCMs were suspended in solutions, lowering pH below a critical value resulted in transition from LBCM to SBCM micelles, while lowering temperature below PNIPAM's LCST resulted in disintegration of micellar cores and dissolution of BCMs to PDMA-*b*-PNIPAM unimers.[36] Qualitatively, changes in Figure 2a−c are consistent with this trend. At lower pH values, as the PDMA coronae became highly ionized (pK_a of PDMA is 6.8), the average lateral radius of micellar surface aggregates decreased from 60 ± 15 to 25 ± 6 nm, which indicated the pH-induced micellar restructuring. Note that the surface micellar aggregates, however, are likely to have aggregation numbers different from those for SBCM existing in solution at pH 4. In contrast, upon exposure of LBCM monolayers to aqueous solution at the same pH but a lower temperature, 25 °C, rms roughness of LBCM monolayers decreased from 2.0 ± 0.4 to 0.4 ± 0.1 nm, indicating disintegration of LBCM cores and likely formation of a PDMA-*b*-PNIPAM brushlike layer, in which PDMA block is bound to the precursor layer and PNIPAM chains are exposed to the solution. After application of pH and temperature stimuli, the dry film thickness remained at 4.0 ± 0.3 nm (Figure 2d). Considering that ellipsometric measurements reflect the average thickness and adsorbed mass of the film within ~1 mm^2 area,[39] this result suggests no loss of polymer chains in solution. Figure S2 shows that drying had no significant effect on the morphology of the LBCM monolayer adsorbed from pH 6 at 45 °C. In both cases, stimuli-induced restructuring may occur through local rearrangements and binding to neighboring available PSS units of the precursor layer as well as through direct dissociation of LBCM into unimers and their reassembly to smaller micelles at the surface. However, unlike fast restructuring in solution, where micelle-to-micelle transition was complete after 5 min of the application of the pH trigger,[36] several hours were required to reach stable micellar morphology at surfaces. Figure S3 shows that morphological changes were complete only after ~4 h, as indicated by evolution of rms roughness (Figure S3d). "Wet" AFM measurements of LBCM monolayer restructuring in Figure S4 show a trend of surface smoothing on a time scale consistent with the data for dry LBCM monolayers in Figure S3. Obviously, binding of BCM coronal chains with the surface dramatically slowed the kinetics of pH-induced micellar restructuring. Figure S5 in the Supporting Information shows that, unlike in solution, micellar restructuring occurred irreversibly within a monolayer; the original micellar surface morphology did not recover after 4 h reversal of pH or temperature stimuli. Moreover, we found that original surface morphologies and rms roughness did not return to their original values even after 2 day immersion in solutions where pH was changed back to 6. Note that a very different behavior, i.e., reversible "opening" and "closing" of micelles ("surface anemones"), was demonstrated earlier for monolayers of micelles with pH-responsive cores at mica, where micelles were weakly anchored to the surface by a small number of ionic bonds.[42] In our case, strong pinning of PDMA coronal chains to PSS in precursor layer inhibited re-forming of PDMA-*b*-PNIPAM LBCM surface micelles.

Figure 3 shows that coating of PSS on top of LBCM monolayers drastically changed film response to both pH and temperature.

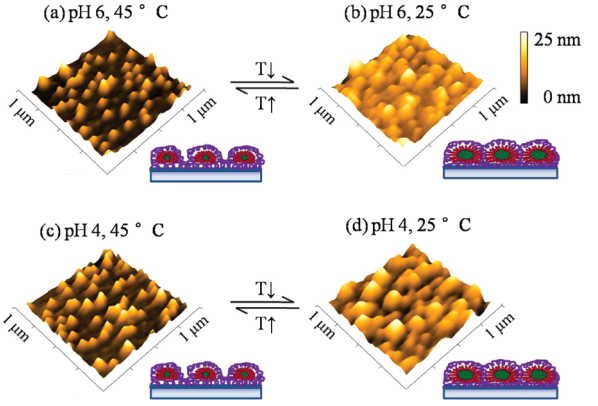

Figure 4. Surface morphology of wet LBCM/PSS single bilayer films with dry thickness of 5.2 ± 0.4 nm after 5 min exposure to 0.01 M phosphate buffer solutions at (a) pH 6, 45 °C, (b) pH 6, 25 °C, (c) pH 4, 45 °C, and (d) pH 4, 25 °C observed by *in situ* AFM.

The LBCM/PSS bilayer film deposited at pH 6 preserved its morphology after exposure to buffer solutions at pH 4 (Figure 3b) or 25 °C (Figure 3c) for as long as 4 and 24 h (data not shown). The suppressed pH and temperature responses of LBCM micelles are easily understood as a result of compensation of PDMA charge as well as structural inhibition of micellar rearrangements by strongly bound PSS chains. Similar "freezing" of pH- and temperature-induced restructuring occurred in the bilayer of SBCM deposited at pH 4 and 45 °C (see Figure S7 in the Supporting Information). The inhibition of surface restructuring within BCM/PSS bilayer films is explained by strong binding between PDMA coronal chains and PSS. Dubas and Schlenoff estimated free energy of segmental interaction of a similar polycation, poly(diallyldimethylammonium chloride), with PSS, $\Delta G°$ as -8.0 kJ mol^{-1} (or ~3 kT per ionic pair at 300 K).[43] This estimate of interaction energy of polyelectrolyte segment pairs has been done for standard conditions, i.e., for 1 M NaCl solutions. At low concentrations of small ions used in our experiment, even higher energy of segmental pairing is expected. An additional increase in the binding energy in our case might also result from the fact that PDMA contains less sterically restricted tertiary amino groups as compared to quaternary amino groups in poly(diallyldimethylammonium chloride). Estimating that up to 15 monomeric units of PSS might be involved in a single binding event with BCMs (based on electrostatic persistent length of PSS in 0.1 mM NaCl of ~40 nm[44]), the activation energy for rearrangements of BCM/PSS contacts can be estimated as up to 45 kT. Our experiments show that this activation energy cannot be overcome by the stress originating from the temperature-triggered expansion of PNIPAM cores of adsorbed PDMA-*b*-PNIPAM BCMs.

Swelling of BCM/PSS Assemblies. Since insensitivity of morphology of BCM/PSS films to changes in pH and temperature in the dry state does not preclude morphological and swelling changes in the wet state, we then sought to probe pH and temperature responses of BCM/PSS assemblies in aqueous solution. In the case of LBCM/PSS bilayers, measurements of film swelling using phase-modulated ellipsometry could not be performed because of large uncertainty associated with decoupling film refractive index and film thickness for such a thin film.[45] The surface morphology of LBCM/PSS bilayer films was therefore first visualized by *in situ* AFM. Figure 4 shows that micellar morphology is

(42) Webber, G. B.; Wanless, E. J.; Armes, S. P.; Tang, Y. Q.; Li, Y. T.; Biggs, S. *Adv. Mater.* **2004**, *16*, 1794.

(43) Dubas, S. T.; Schlenoff, J. B. *Langmuir* **2001**, *17*, 7725.
(44) Degiorgio, V.; Mantegazza, F.; Piazza, R. *Europhys. Lett.* **1991**, *15*(1), 75.
(45) Pristinski, D.; Kozlovskaya, V.; Sukhishvili, S. A. *J. Opt. Soc. Am. A* **2006**, *23*, 2639.

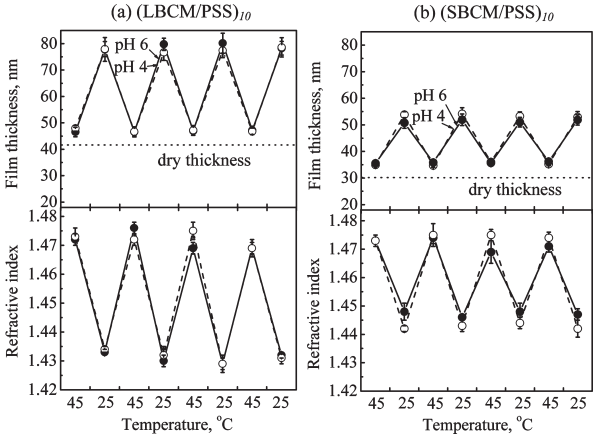

Figure 5. Reversible temperature-induced swelling of $(LBCM/PSS)_{10}$ (left, panel a) and $(SBCM/PSS)_{10}$ (right, panel b) films in 0.01 M phosphate buffer solutions at pH 6 (filled circles) and pH 4 (open circles), respectively, measured by *in situ* ellipsometry with alternating 5 min film incubations in 45 or 25 °C solutions. Dotted horizontal lines show thicknesses of dry $(LBCM/PSS)_{10}$ and $(SBCM/PSS)_{10}$ films.

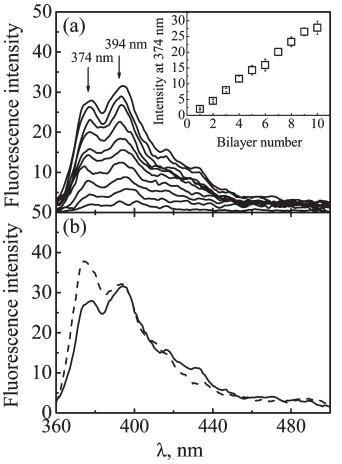

Figure 6. (a) Representative fluorescence spectra (main panel) and average fluorescent intensity at 374 nm collected from three spots on the same film (inset) of a dry $(LBCM^{pyr}/PSS)_n$ film as a function of bilayer number. (b) Comparison of fluorescence spectra of the dry $(LBCM^{pyr}/PSS)_{10}$ film (solid line) and pyrene aqueous solutions fluorescence after 5 h release into aqueous solution at pH 6, 45 °C (dashed line). All spectra were collected using the excitation wavelength at $\lambda_{ex} = 333$ nm.

retained within wet BCM/PSS films after the application of both pH and temperature stimuli. However, in contrast to morphology of dry BCM/PSS assemblies that was equally unaffected by environmental stimuli (Figure 3), the effects of pH and temperature on the size of wet surface micelles were distinctly different. While variations in pH did not significantly change wet film morphology (Figure 4a,c), lowering temperature below PNIPAM's LCST led to an increase in the average radius of micelles in LBCM/PSS films from 60 ± 15 nm (Figure 4a,c) to 140 ± 35 nm (Figure 4b,d), reflecting swelling of micellar features. These changes illustrate an uptake of water within PNIPAM cores as PNIPAM blocks become hydrophilic and soluble below PNIPAM's LCST. Temperature-induced changes in morphology of wet LBCM/PSS films were fully reversible. Interestingly, morphological changes during multiple drying/wetting cycles were very robust and recovered the consistent morphology and roughness for wet and dry states (shown in Figures 4b and 3c, respectively) after three repeated cycles.

We then proceeded to study multilayered BCM/PSS assemblies. Figure S8 illustrates a linear increase in dry film thickness during the deposition of LBCM (or SBCM)/PSS multilayer films. PSS layer was always included as the top film layer. The linear increase in film thickness in Figure S8a indicates robust growth of LBCM (SBCM)/PSS films within no competitive displacement of adsorbed micelles during film deposition. As discussed above, single monolayers of micelles did not cover the surface completely. High surface coverage with LBCMs was achieved after depositing two LBCM/PSS bilayers, and during further film growth the surface roughness increased (Figure S8b−d) from 2.4 ± 0.3 nm to 3.2 ± 0.4 and 5.3 ± 0.8 nm for 1-, 2-, and 4-bilayer LBCM/PSS films, respectively. With $(LBCM/PSS)_{10}$ and $(SBCM/PSS)_{10}$ films, dry ellipsometric thicknesses of 42.0 ± 1.7 and 31.2 ± 1.8 nm have been achieved, respectively, enabling the application of phase-modulated ellipsometry to assess film swelling.[45]

Figure 5 illustrates swelling of $(LBCM/PSS)_{10}$ and $(SBCM/PSS)_{10}$ films as a function of solution temperature as determined by *in situ* ellipsometry. $(LBCM/PSS)_{10}$ film swelled by ~10% from its dry thickness of 42.0 ± 1.7 nm when exposed to buffer solution at 45 °C. This swelling was accompanied by a change in refractive index from 1.5 for dry film to 1.43 for wet film. A much larger (~65%) increase in film swelling occurred when $(LBCM/PSS)_{10}$ film was immersed in the same buffer solution at 25 °C, presumably due to the expansion of micellar cores as a result of water uptake. Swelling/deswelling of $(LBCM/PSS)_{10}$ film was fully reversible and could be repeated over at least 4 cycles (Figure 5a). Similarly, $(SBCM/PSS)_{10}$ films also demonstrated temperature-controlled swelling transitions in aqueous solutions (Figure 5b). Films swelled by a similar percentage of ~9% and ~60% of dry thickness of 31.2 ± 1.8 nm upon exposure to 0.01 M phosphate buffer solutions at 45 and 25 °C, respectively. In the above experiments, the film exposure time to solutions with controlled temperature was a relatively short time 5 min. However, our control experiments in which films were exposed to 25 °C for a longer time 1 h showed that the swelling ratio did not change between 5 min and 1 h exposure times, and the film swelling response remained fully reversible (data not shown). The data are also consistent with data in Figure 3, showing that LBCM/PSS bilayer films did not restructure after 4 h application of pH and/or temperature stimuli. Fast swelling response of the films and the absence of longer term changes in film swelling suggest fast "yielding" of PSS/micellar coronal ionic network to swelling and collapse of PNIPAM micellar cores, with no, or negligible, rearrangements of PSS/PDMA ionic contacts. Finally, Figure 5 also shows that film swelling is almost independent of postassembly solution pH—a result expected in view of neutralization of coronal micellar charge by PSS. The reversible, temperature-triggered, pH-independent swelling seen in Figure 5 is central to future applications of these films for controlled delivery of functional molecules from surfaces.

BCM/PSS Multilayers: Temperature-Controlled Diffusion of Pyrene. We have exploited the capability of pyrene to partition into hydrophobic environments and studied temperature-dependent retention of dye within micellar PNIPAM cores. Prior to film deposition, LBCMs were preloaded with pyrene as described in the Experimental Section. Film deposition at 45 °C was then followed by measuring fluorescence intensity of the dry multilayer film. Figure 6a shows evolution of fluorescence spectra of dry $LBCM^{pyr}/PSS$ multilayer films with number of deposited bilayers. The fluorescence intensity ratio of two pyrene emission peaks at 374 and 394 nm, I_{374}/I_{394}, was ~0.9, i.e., lower than that

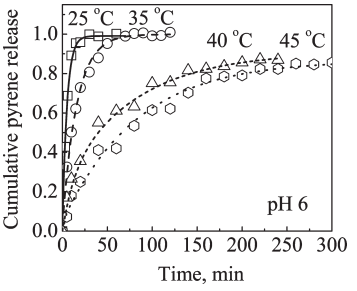

Figure 7. Release profile of pyrene dye from $(LBCM^{pyr}/PSS)_{10}$ film in 0.01 M phosphate buffer solution at pH 6 as followed by the intensity at 374 nm with excitation wavelength of $\lambda_{ex} = 333$ nm. pH of aqueous solutions was adjusted to 6, and temperature was controlled at 25 °C (squares), 35 °C (circles), 40 °C (triangles), and 45 °C (hexagons). The data were normalized to the fluorescence intensity of pyrene solutions collected after a completion of pyrene release from the $(LBCM/PSS)_{10}$ films in pH 6 0.01 M phosphate buffer solution at 25 °C.

of aqueous pyrene solutions (~1.2), suggesting inclusion of pyrene within hydrophobic environment of the film. Also note the absence of an emission band at 475 nm associated with pyrene excimers. From the density of micelles on the surface and the increase of fluorescence intensity of the solution after pyrene release, we estimated the loading capacity of pyrene within $(LBCM^{pyr}/PSS)_{10}$ film as 3×10^3 dye molecules per micelle, or 0.65 mg/m^2 of the multilayer film. The calculated dye loading capacity of micelles is within the 1100−3500 dye/micelle range reported by others.[17,34,46]

As shown in the inset of Figure 6a, the fluorescence intensity increased in a linear fashion with number of bilayers within the film, suggesting robust film deposition and retention of pyrene by micelles during film deposition.

Constructed $(LBCM^{pyr}/PSS)_{10}$ films were then immersed in 0.01 M phosphate buffer solution at different pH and temperature, and dye release was measured by fluorescence intensity at 374 nm of buffer solution in contact with the multilayer films. Figure 6b shows that I_{374}/I_{394} ratio of fluorescent intensity for pyrene detected in solution changes significantly (increasing from 0.9 to 1.2) as pyrene's environment changes from hydrophobic, within the film, to hydrophilic in aqueous solution.[47,48] Figure 7 shows kinetics of pyrene release into buffered water at pH 6 from $(LBCM^{pyr}/PSS)_{10}$ films. Clearly, the rate of pyrene release was higher at 25 and 35 °C than at temperatures above PNIPAM's LCST, e.g., 40 and 45 °C. At 40 and 45 °C, the half-time of dye release was 50 and 70 min, respectively. The relatively low release rate of pyrene is likely due to strong interactions between pyrene and collapsed hydrophobic PNIPAM cores. At temperatures lower than LCST of PNIPAM block (37 °C for $PDMA_{57}$-*b*-$PNIPAM_{97}$), PNIPAM cores became hydrophilic, resulting in weaker binding of pyrene with BCMs as shown in Figure S9. Note that at 40 and 45 °C ~90% of the total amount of loaded pyrene was released in solution, while the remaining 10% was irreversibly trapped within LBCM/PSS films. The incomplete release of dye is due to partial trapping within hydrophobic BCM cores as well as within hydrophobic domains created by interacting PDMA and PSS chains and is consistent with previous reports.[34,46] In a control experiment with 10-bilayer films of PDMA-*b*-PNIPAM copolymer assembled with PSS at 25 °C when the copolymer existed as unimers, we showed that the amount of pyrene loaded in these micelle-free films was ~12% of the amount of pyrene loaded in $(LBCM^{pyr}/PSS)_{10}$ films, suggesting that irreversibly trapped pyrene was probably included within hydrophobic domains of the film created after changing neutralization between PDMA coronal chains and PSS. In Figure 7, all fluorescence intensities of pyrene solutions were normalized to the limiting fluorescence intensity collected after completion of dye release from $(LBCM/PSS)_{10}$ film in 0.01 M phosphate buffer solution at 25 °C. As shown in Figure 7, in a relatively narrow temperature range of 5 deg (a change from 40 to 35 °C), the half-time of pyrene release decreased from 50 to 10 min, respectively. This trend is opposite to an expectation that temperature usually speeds up diffusion. Unlike the effect of temperature on freely diffusing species, diffusion of dye from film in Figure 7 was controlled by the dye's partitioning in the micellar cores. Importantly, the film could be reloaded with pyrene dye and reused for the release experiments, with only 10% decrease in film loading capacity after four repeated temperature cycles. Such film robustness, stabilized exclusively by noncovalent interactions, is consistent with data in Figures 3 and 4. The dye release rate was also affected by solution pH, but the effect of pH was much weaker than that of temperature (Figure S10). As in the case of temperature-triggered release, films could also be reloaded with dye and reused for pH-dependent release experiments.

Conclusion

We studied temperature- and pH-responsive properties of diblock copolymer micelles containing polyelectrolyte and temperature-responsive blocks, when such micelles were self-assembled at surfaces. When in solution, such micelles were reported earlier to demonstrate a phase transition between micelles of larger and smaller aggregation number in response to pH variation or disassemble in response to temperature. At surfaces, the mode of film response was strongly dependent on whether such micelles resided at the surface as a single monolayer or were self-assembled with a polyanion, such as PSS. In a single monolayer, BCMs changed their aggregation number in response to pH variations, only slowly and irreversibly, in contrast to their fast reversible restructuring in solution. When assembled with PSS, BCMs demonstrated inhibition of pH response, while retaining response to temperature. Robust and reversible swelling transitions caused by collapse/hydration of micellar cores were observed with BCM/PSS films. While similar temperature-induced swelling transitions were observed with hydrogen-bonded films of nonionic BCMs,[34] or with electrostatically assembled layers of triblock copolymer micelles,[35] this finding demonstrates the responsive behavior of assemblies of ionic diblock copolymers. In the future, it will be interesting to explore the effect of the molecular weight of PSS or other polyanions on the pH and temperature responses of BCM films. Envisioned applications of such films include actuation at nanoscale as well as controlled adhesion and adsorption/release of functional molecules at surfaces.

Acknowledgment. This work was supported by the National Science Foundation under Awards DMR-0710591 and DMR-0906474. The authors also thank Aliaksandr Zhuk for helpful discussions.

Supporting Information Available: AFM images of SBCM/PSS films. This material is available free of charge via the Internet at http://pubs.acs.org.

(46) Addison, T.; Cayre, O. J.; Biggs, S.; Armes, S. P.; York, D. *Langmuir* **2008**, *24*, 13328.
(47) Kalyanasundaram, K.; Thomas, J. K. *J. Am. Chem. Soc.* **1977**, *99*, 203.
(48) Lee, A. S.; Gast, A. P.; Bütün, V.; Armes, S. P. *Macromolecules* **1999**, *32*, 4302.